# Electronic Supplementary Information

## Formation of Unexpected Silicon- and Disiloxane-Bridged Multiferrocenyl Derivatives Bearing Si-O-CH=CH$_2$ and Si(CH$_2$)$_2$C(CH$_3$)$_3$ Substituents via Cleavage of Tetrahydrofuran and Trapping of its Ring Fragments

Sonia Bruña,[a,b] Ana Mª González-Vadillo,[a] Marta Ferrández,[a] Josefina Perles,[c] M. Merced Montero-Campillo,[d] Otilia Mó,[b,d] and Isabel Cuadrado*[a,b]

[a] Departamento de Química Inorgánica, Facultad de Ciencias, Universidad Autónoma de Madrid, Cantoblanco, 28049, Madrid, Spain

[b] Institute for Advanced Research in Chemical Sciences (IAdChem), Universidad Autónoma de Madrid

[c] Laboratorio de Difracción de Rayos X de Monocristal, Servicio Interdepartamental de Investigación (SIdI), Universidad Autónoma de Madrid, Cantoblanco, 28049, Madrid, Spain

[d] Departamento de Química, Facultad de Ciencias, Universidad Autónoma de Madrid, Cantoblanco, 28049, Madrid, Spain

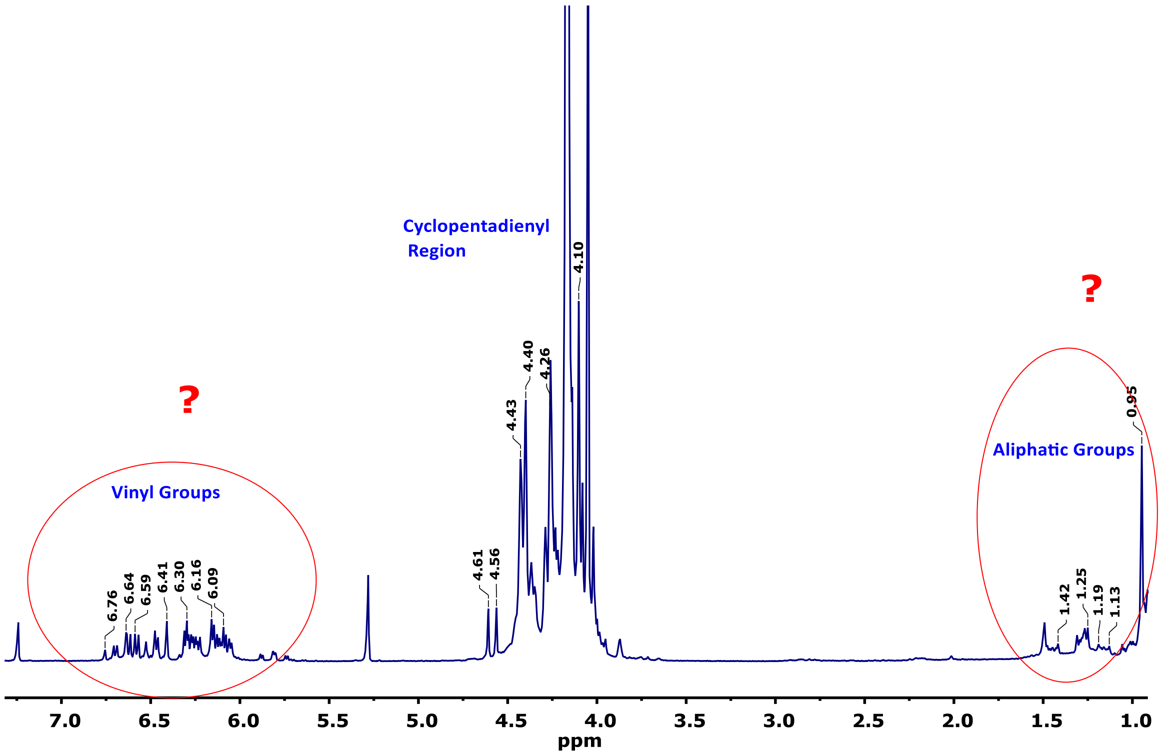

**Figure S1.** $^1$H NMR spectrum of the reaction mixture to obtain **1** following route B.

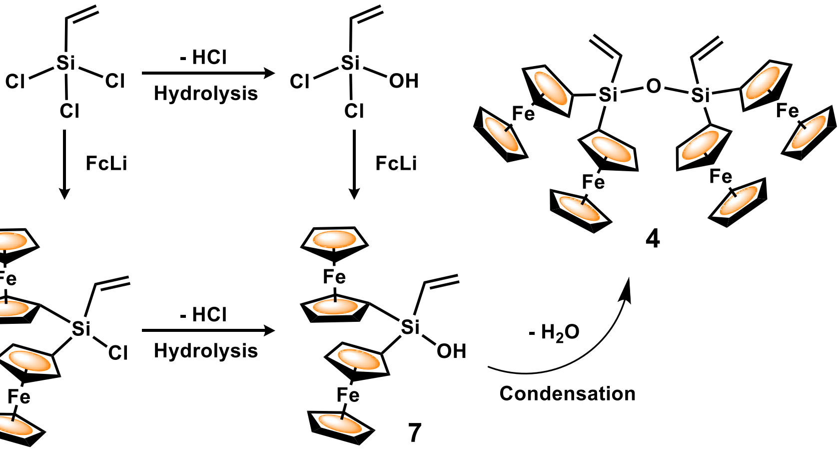

**Scheme S1.** Possible synthetic pathway for the formation of bimetallic silanol **7** and tetrametallic **4**.

## 1. Structural Characterization of Compounds 5-8

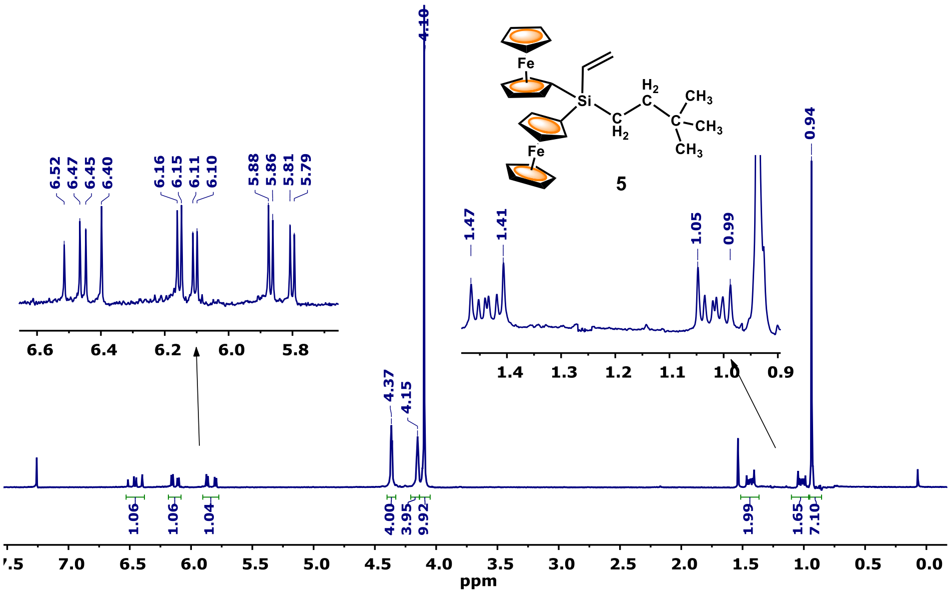

**Figure S2.** $^1$H NMR spectrum (in $CDCl_3$, 300 MHz) of diferrocenyl(3,3-dimethylbutyl)vinylsilane **5**.

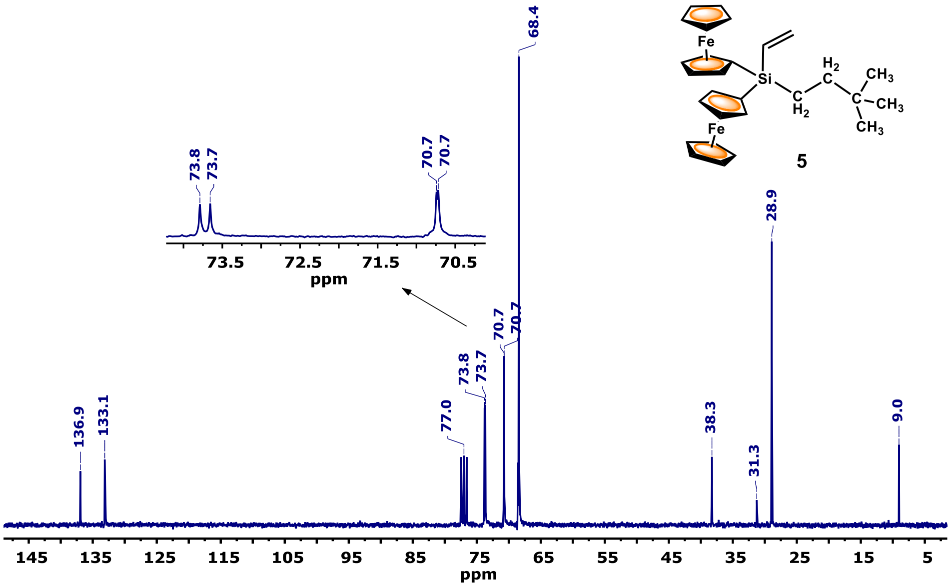

**Figure S3.** $^{13}$C NMR spectrum (in $CDCl_3$, 75 MHz) of diferrocenyl(3,3-dimethylbutyl)vinylsilane **5**.

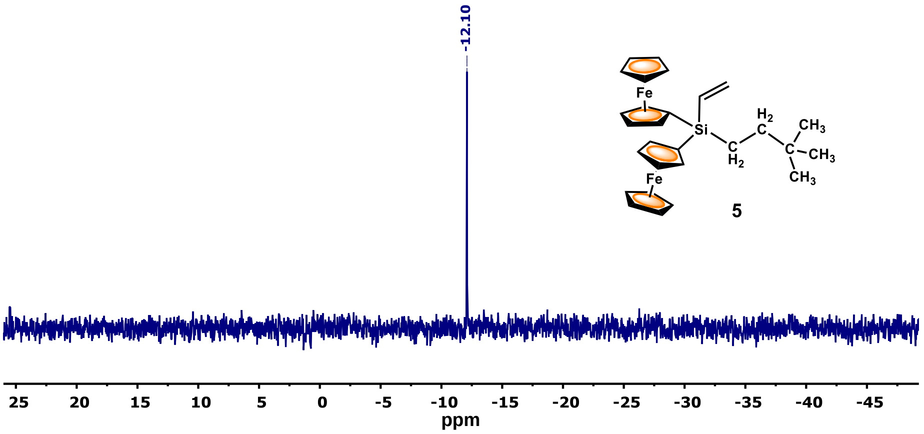

**Figure S4.** $^{29}$Si NMR spectrum (in $CDCl_3$, 59 MHz) of diferrocenyl(3,3-dimethylbutyl)vinylsilane **5**.

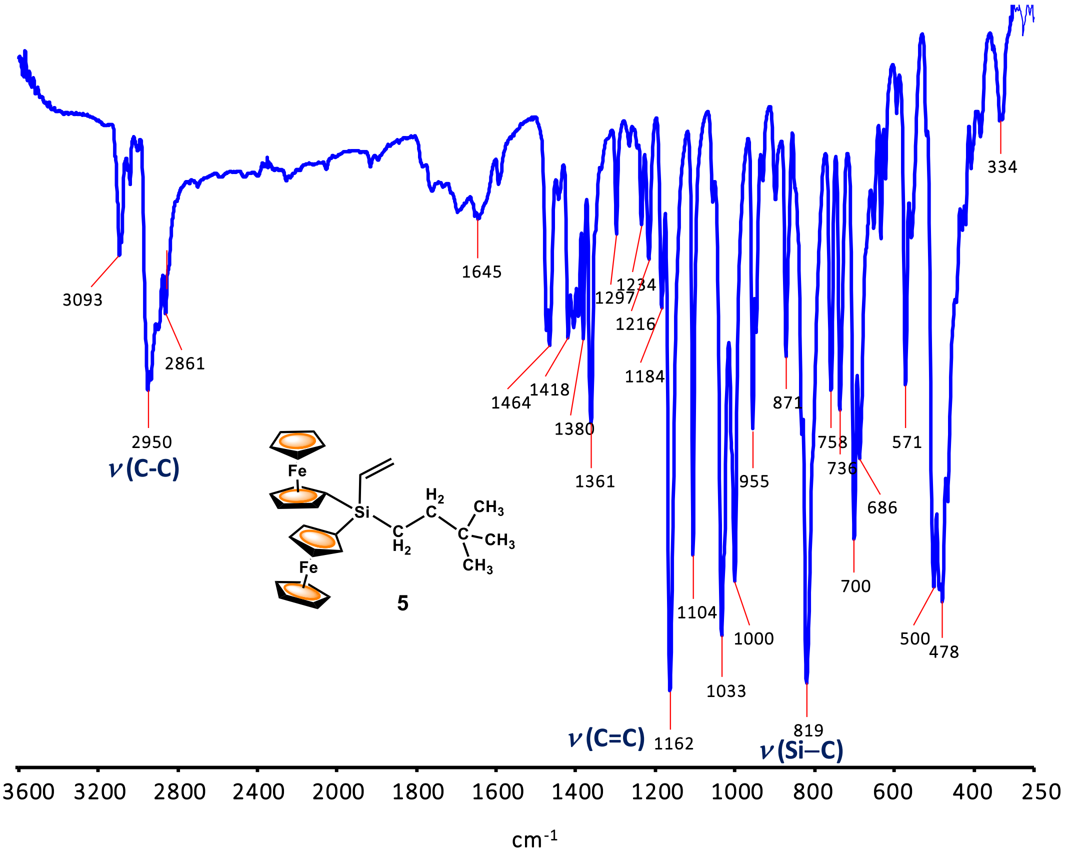

**Figure S5.** IR spectrum (in KBr) of diferrocenyl(3,3-dimethylbutyl)vinylsilane **5**.

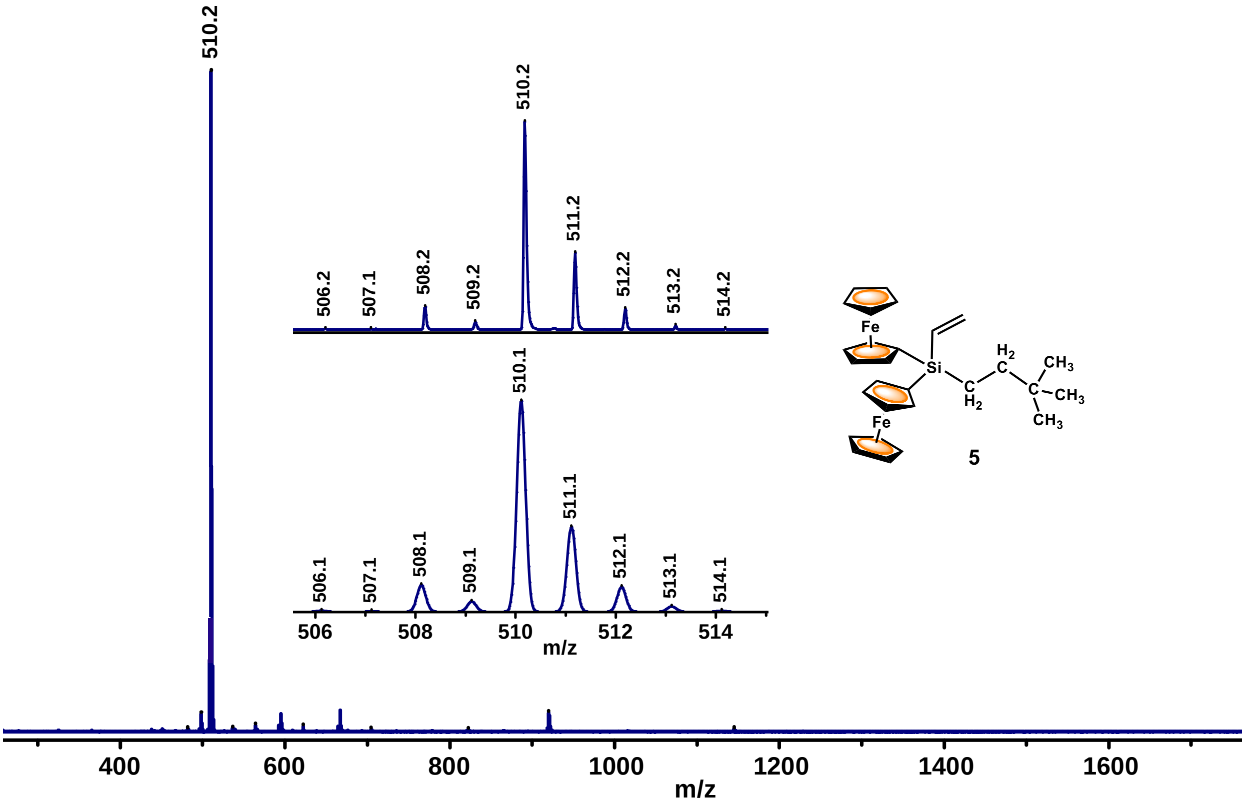

**Figure S6.** Mass spectrometry characterization by MALDI-TOF and experimental (top) and calculated (bottom) isotopic patterns of the [M$^+$] peak for **5**.

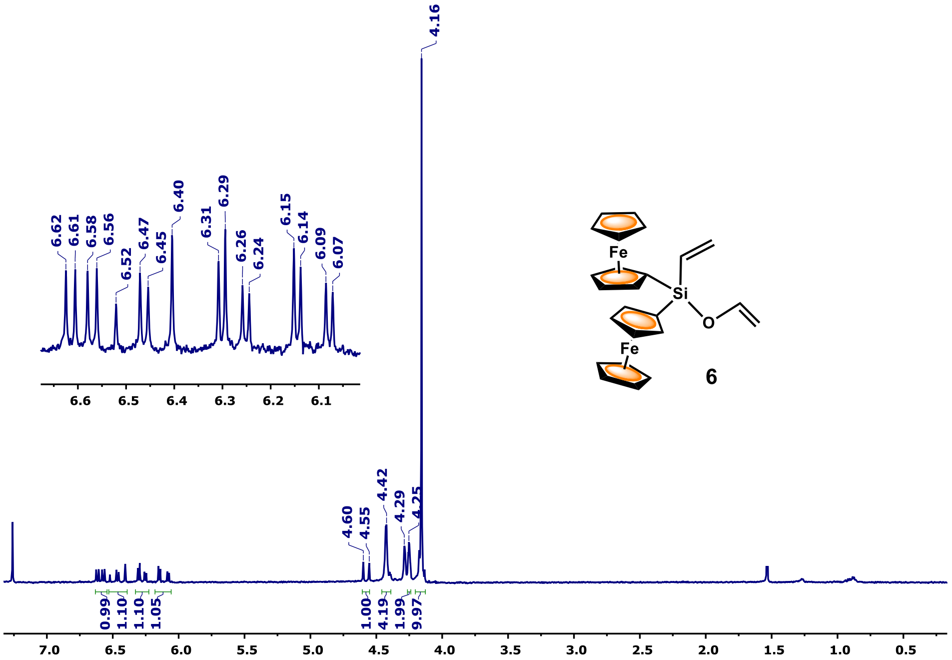

**Figure S7.** $^1$H NMR spectrum (in $CDCl_3$, 300 MHz) of diferrocenylvinyloxyvinylsilane **6**.

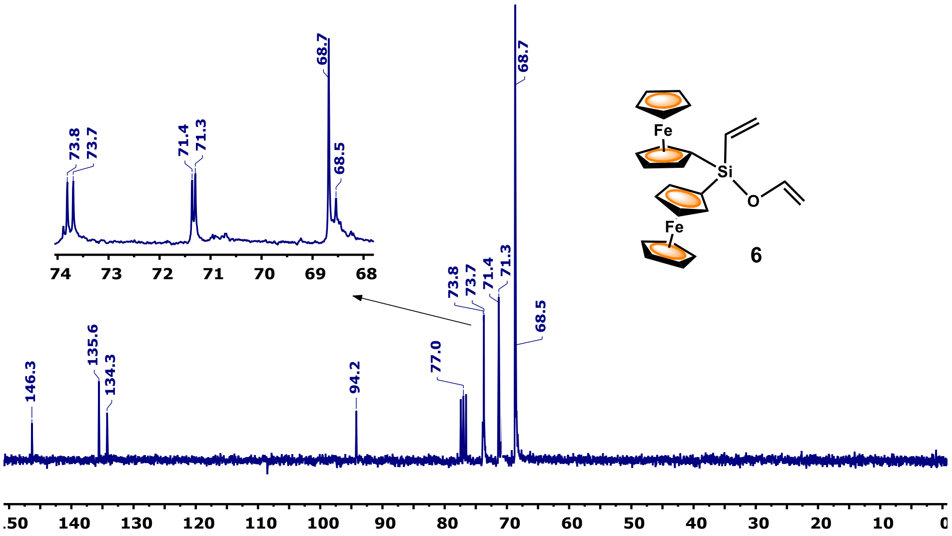

**Figure S8.** $^{13}$C NMR spectrum (in $CDCl_3$, 75 MHz) of diferrocenylvinyloxyvinylsilane **6**.

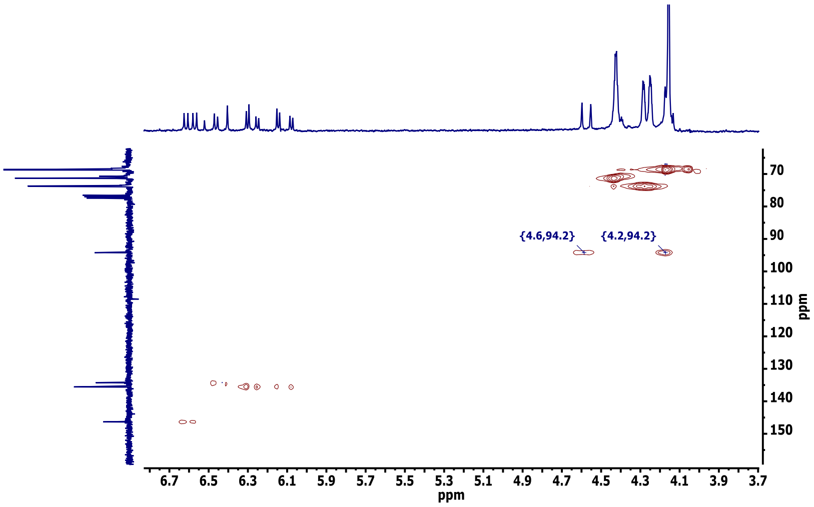

**Figure S9.** {$^1$H–$^{13}$C} HMQC of diferrocenyl **6** ($CDCl_3$, 59 MHz).

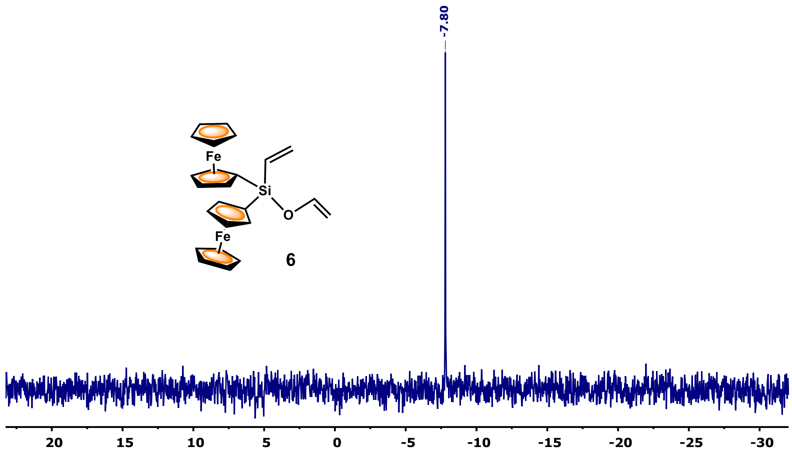

**Figure S10.** $^{29}$Si NMR spectrum (in $CDCl_3$, 59 MHz) of diferrocenylvinyloxyvinylsilane **6**.

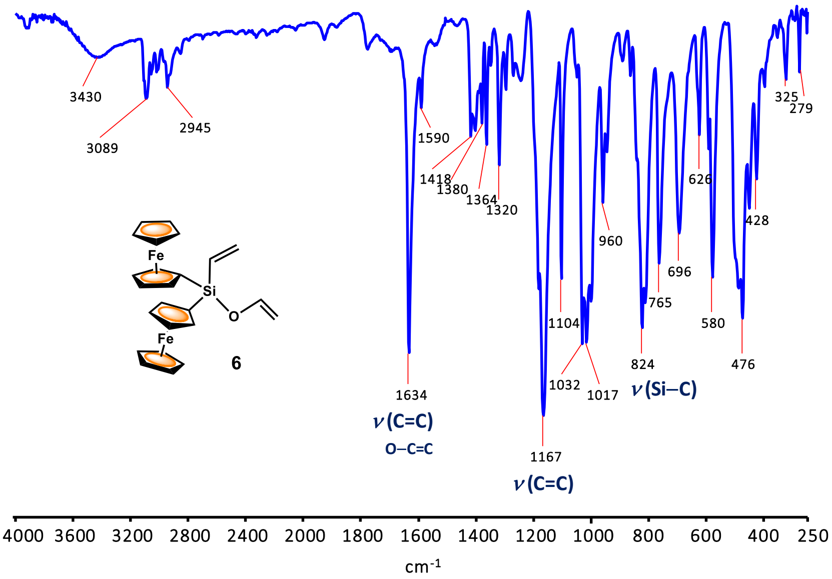

**Figure S11.** IR spectrum (in KBr) of diferrocenylvinyloxyvinylsilane **6**.

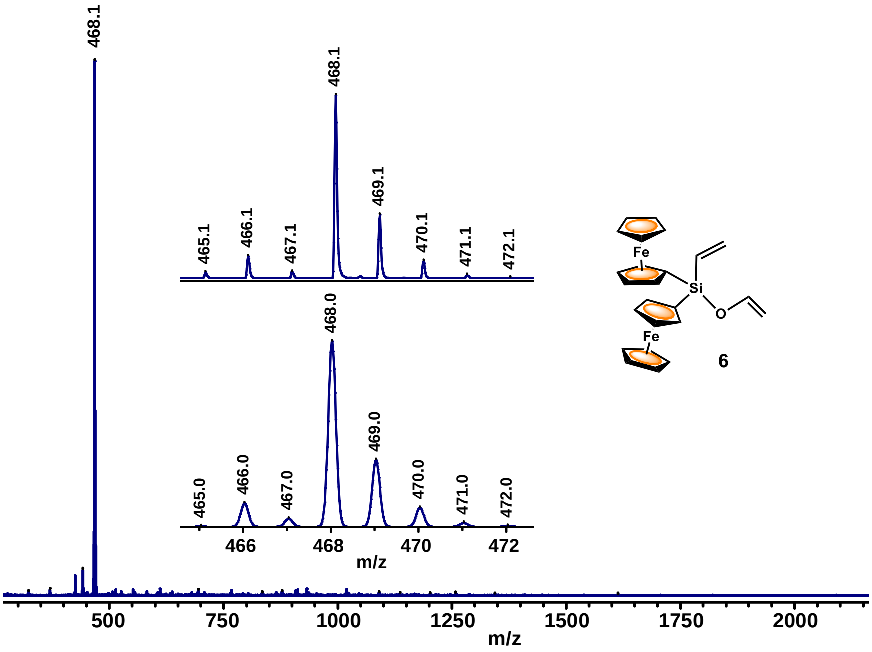

**Figure S12.** Mass spectrometry characterization by MALDI-TOF and experimental (top) and calculated (bottom) isotopic patterns of the [M$^+$] peak for **6**.

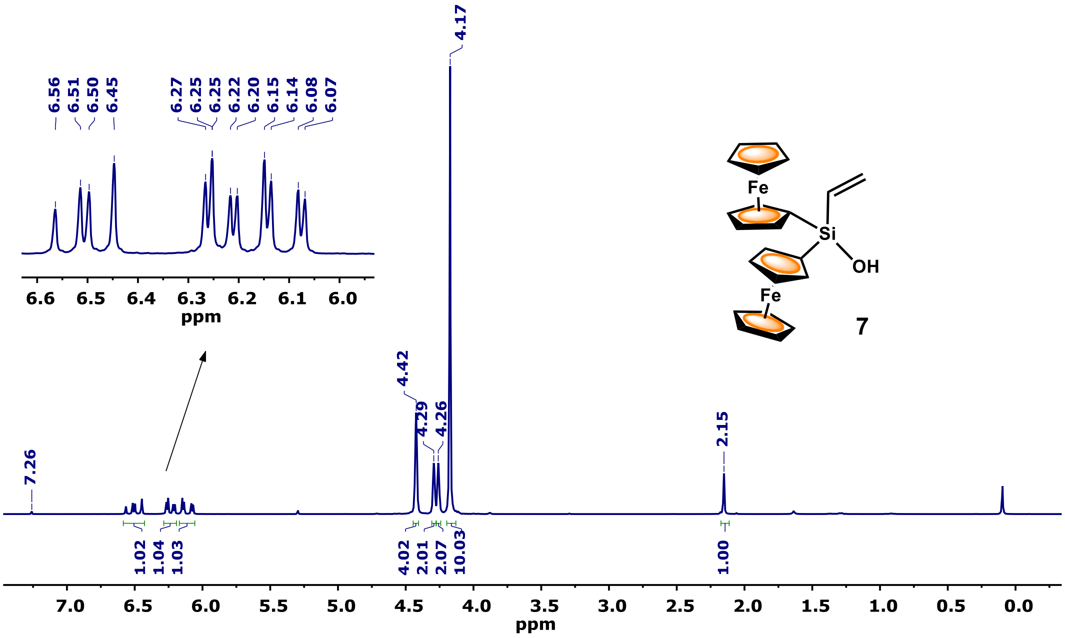

**Figure S13.** $^{1}$H NMR spectrum (in $CDCl_3$, 300 MHz) of diferrocenylvinylsilanol **7**.

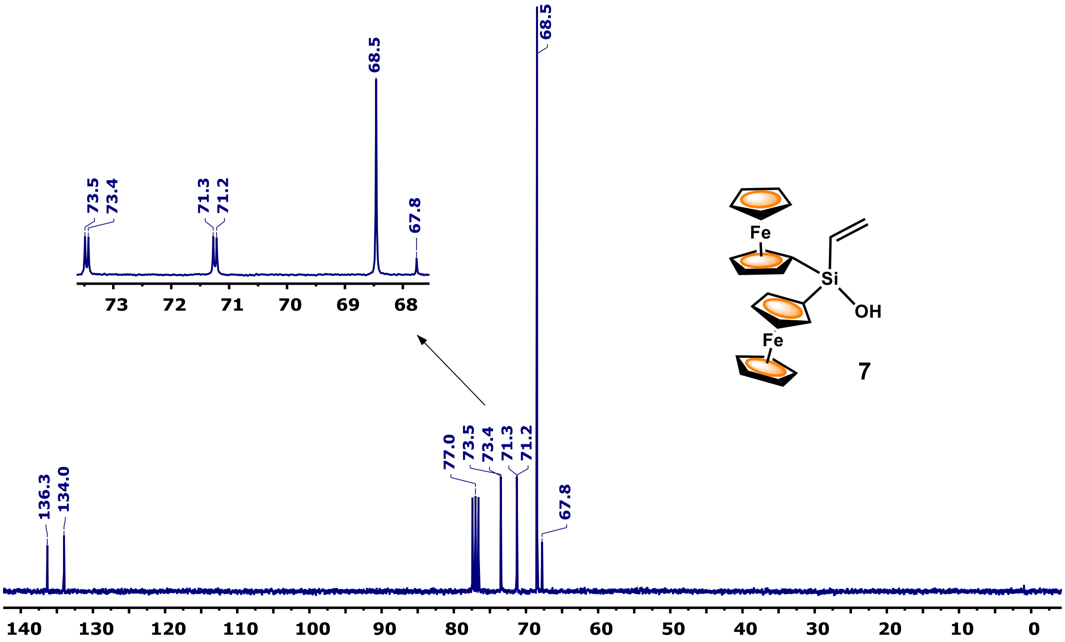

**Figure S14.** $^{13}$C NMR spectrum (in $CDCl_3$, 75 MHz) of diferrocenylvinylsilanol **7**.

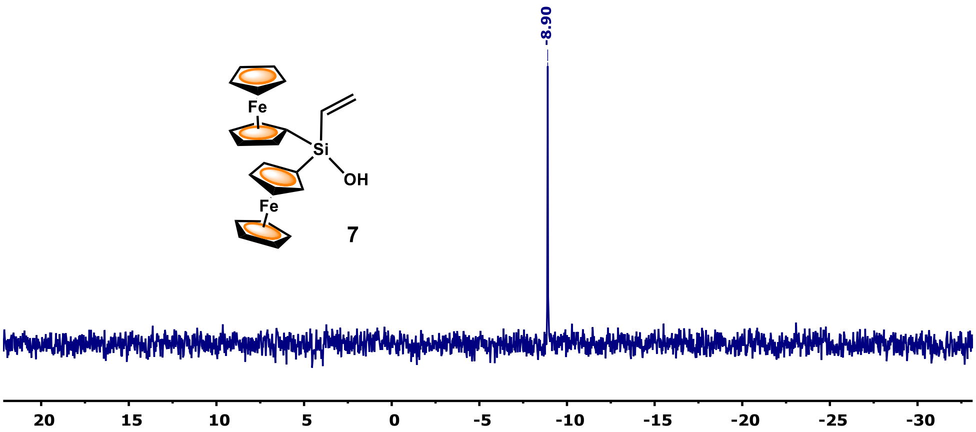

**Figure S15.** $^{29}$Si NMR spectrum (in $CDCl_3$, 59 MHz) of diferrocenylvinylsilanol **7**.

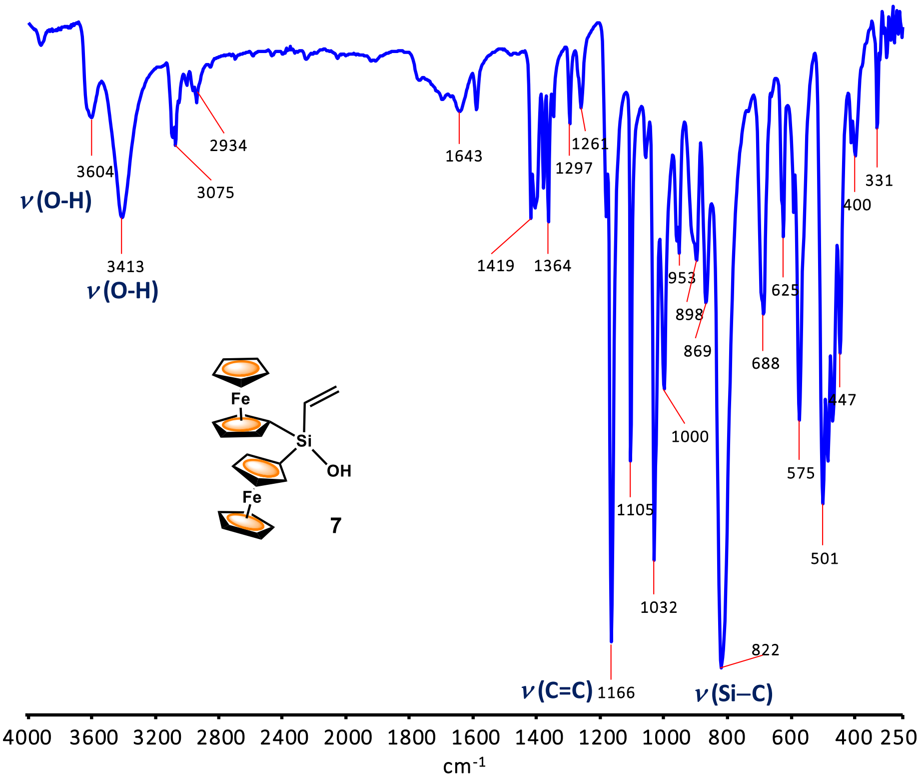

**Figure S16.** IR spectrum (in KBr) of diferrocenylvinylsilanol **7**.

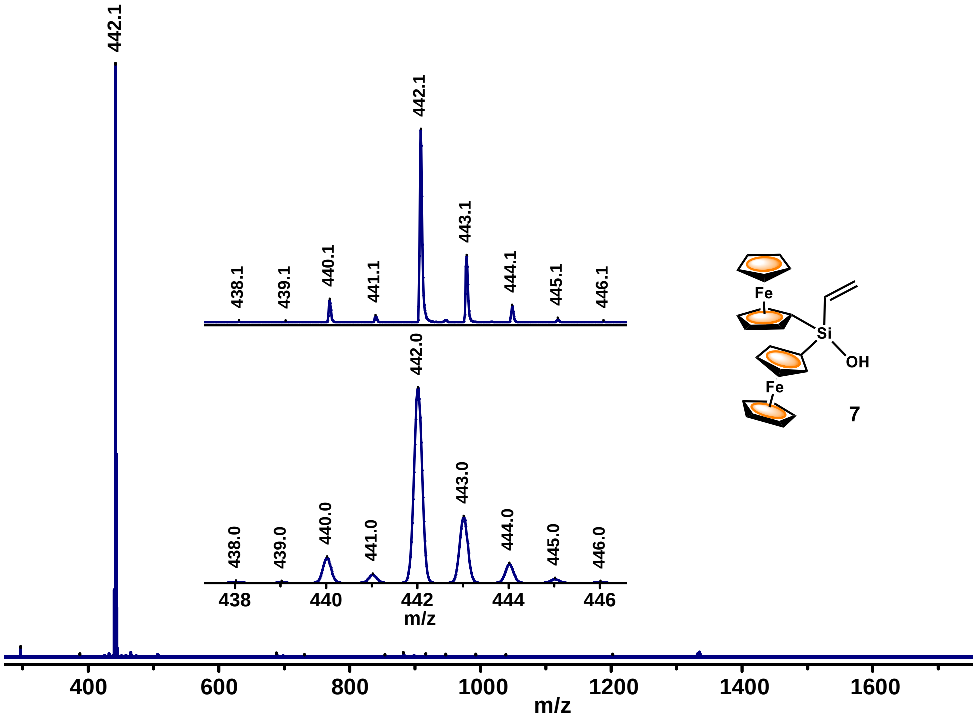

**Figure S17.** Mass spectrometry characterization by MALDI-TOF and experimental (top) and calculated (bottom) isotopic patterns of the [M$^+$] peak for **7**.

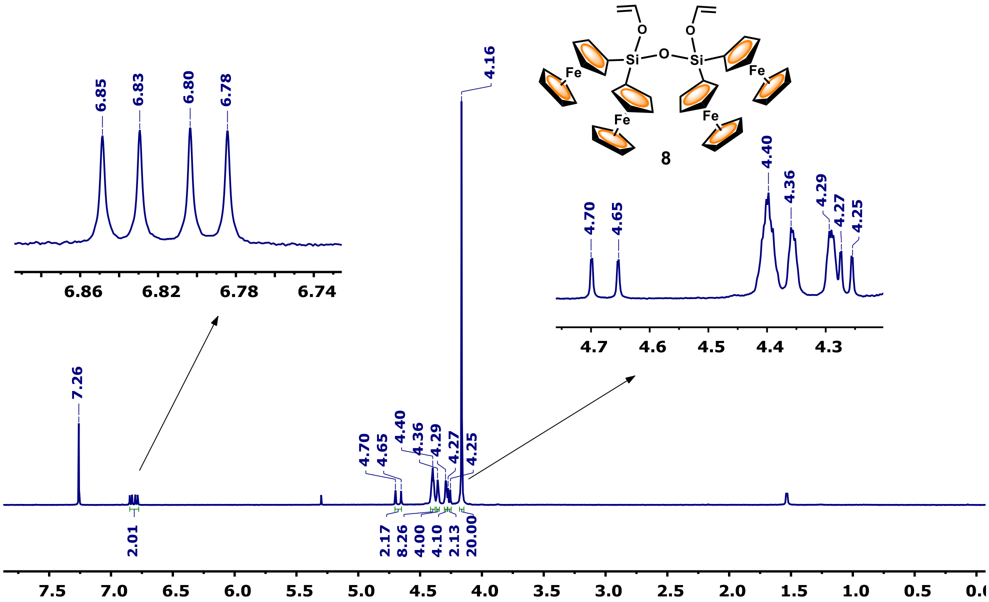

**Figure S18.** $^{1}$H NMR spectrum (in $CDCl_3$, 300 MHz) of tetraferrocenyl disiloxane **8**.

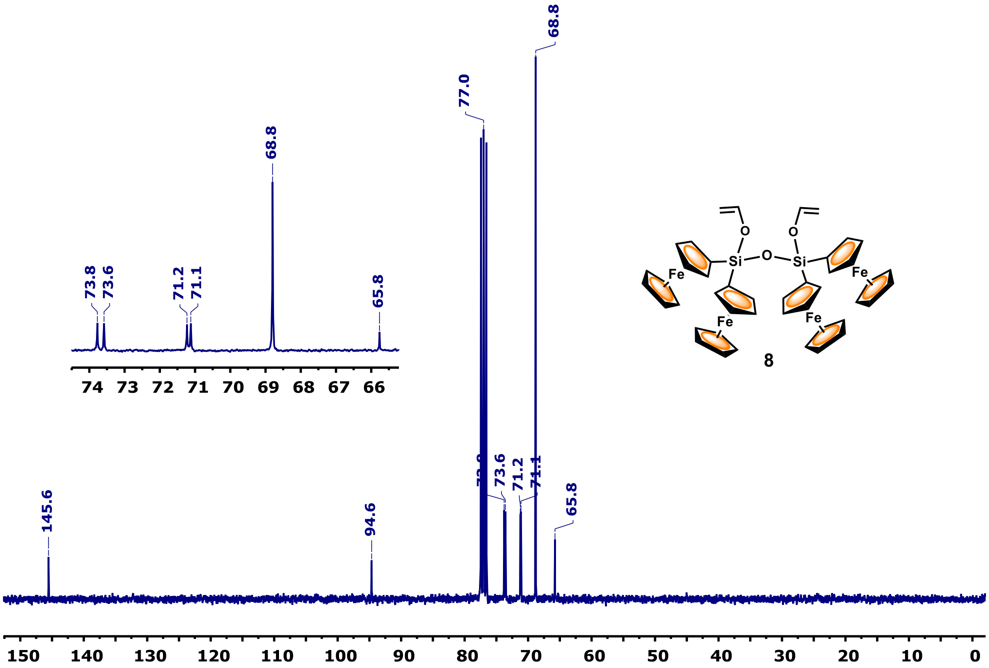

**Figure S19.** $^{13}$C NMR spectrum (in $CDCl_3$, 75 MHz) of tetraferrocenyl disiloxane **8**.

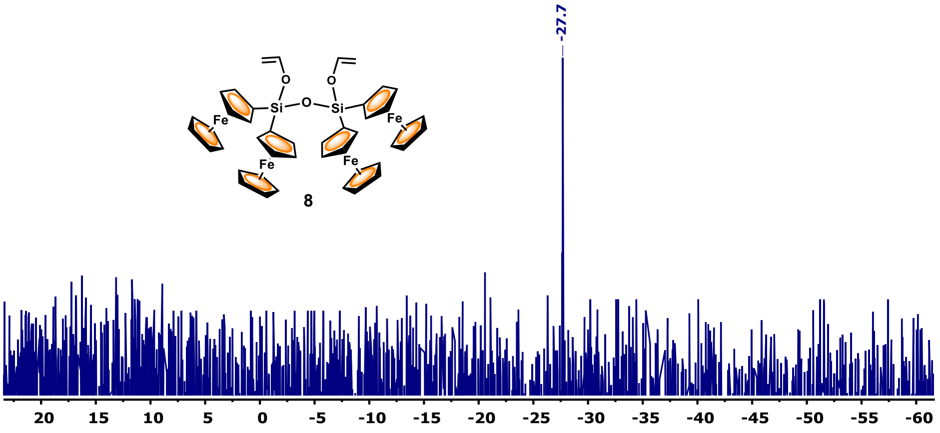

**Figure S20.** $^{29}$Si NMR spectrum (in $CDCl_3$, 59 MHz) of tetraferrocenyl disiloxane **8**.

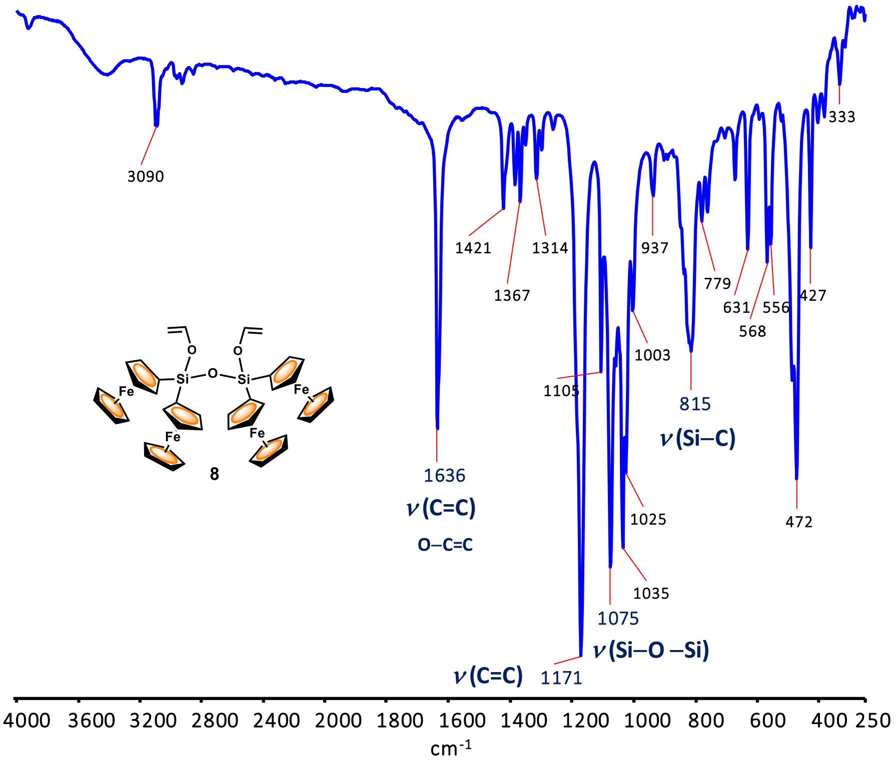

**Figure S21.** IR spectrum (in KBr) of tetraferrocenyl disiloxane **8**.

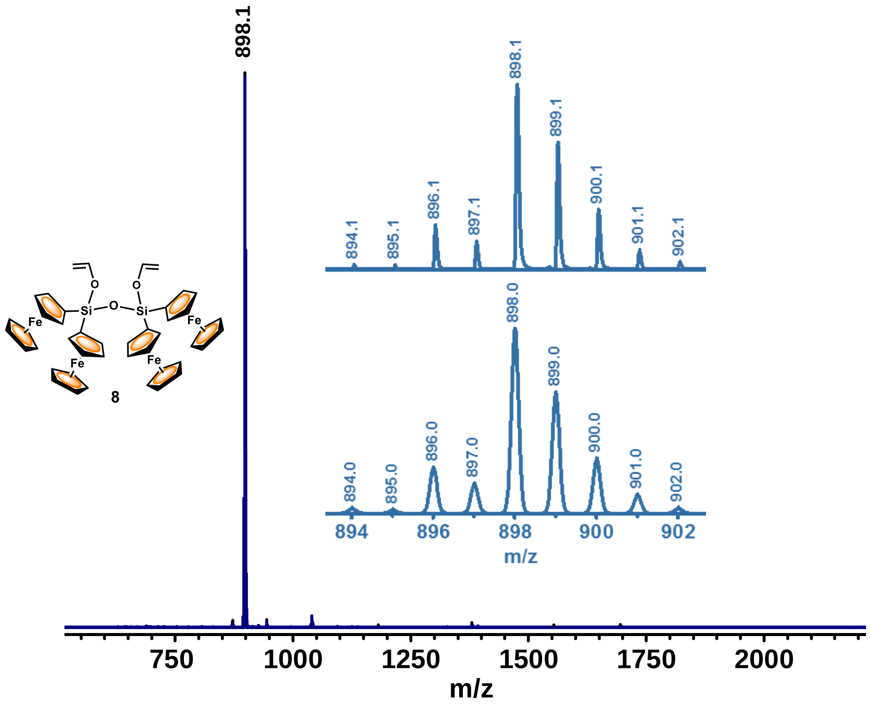

**Figure S22.** Mass spectrometry characterization by MALDI-TOF and experimental (top) and calculated (bottom) isotopic patterns of the [M$^+$] peak for **8**.

## 2. Electrochemical Measurements of Compounds 5-7

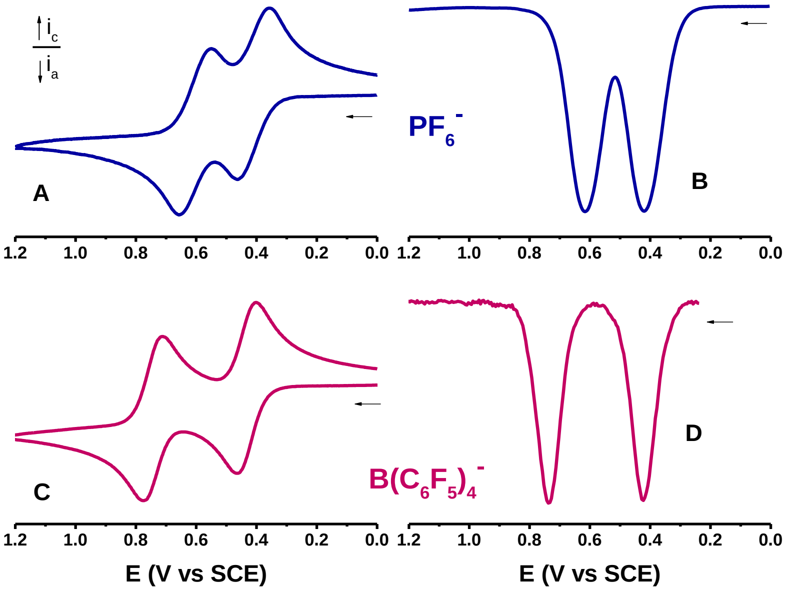

**Figure S23.** CV and SWV responses of compound **5** ($10^{-3}$ M in $CH_2Cl_2$), (A) and (B) containing 0.1 M [*n*-$Bu_4N$][$PF_6$]; (C) and (D) containing 0.1 [*n*-$Bu_4N$][$B(C_6F_5)_4$]. Platinum working electrode.

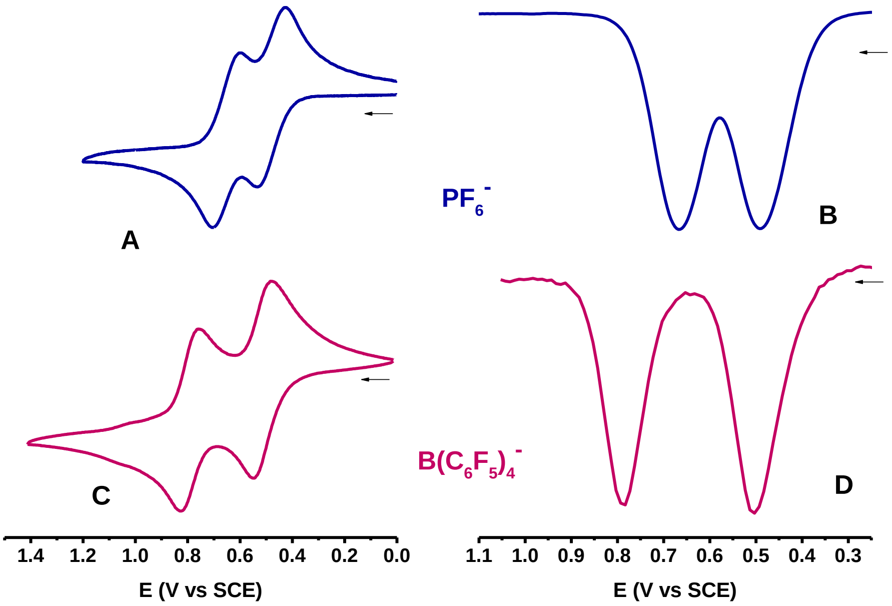

**Figure S24.** CV and SWV responses of compound **6** ($10^{-3}$ M in $CH_2Cl_2$), (A) and (B) containing 0.1 M [*n*-$Bu_4N$][$PF_6$]; (C) and (D) containing 0.1 [*n*-$Bu_4N$][$B(C_6F_5)_4$]. Platinum working electrode.

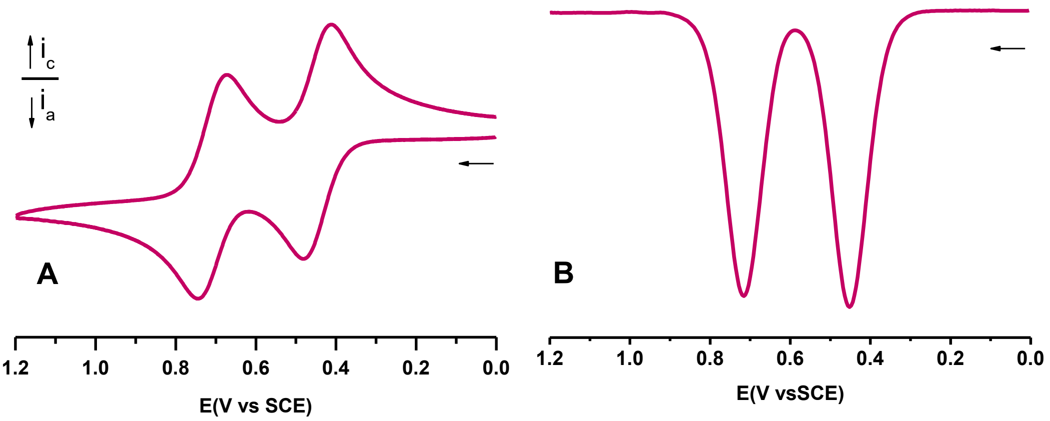

**Figure S25.** CV and SWV responses of compound **7** ($10^{-3}$ M in $CH_2Cl_2$), containing 0.1 [$n$-$Bu_4N$][$B(C_6F_5)_4$]. Platinum working electrode.

## 3. Single Crystal X-Ray Structures of Compounds 5-9

### 3.1. Single crystal X-ray diffraction supplementary information for 5

A clear dark orange prismatic-like specimen of $C_{28}H_{34}Fe_2Si$, approximate dimensions 0.16 mm x 0.18 mm x 0.23 mm, was used for the X-ray crystallographic analysis. The X-ray intensity data were measured in a Bruker Kappa Apex II diffractometer.

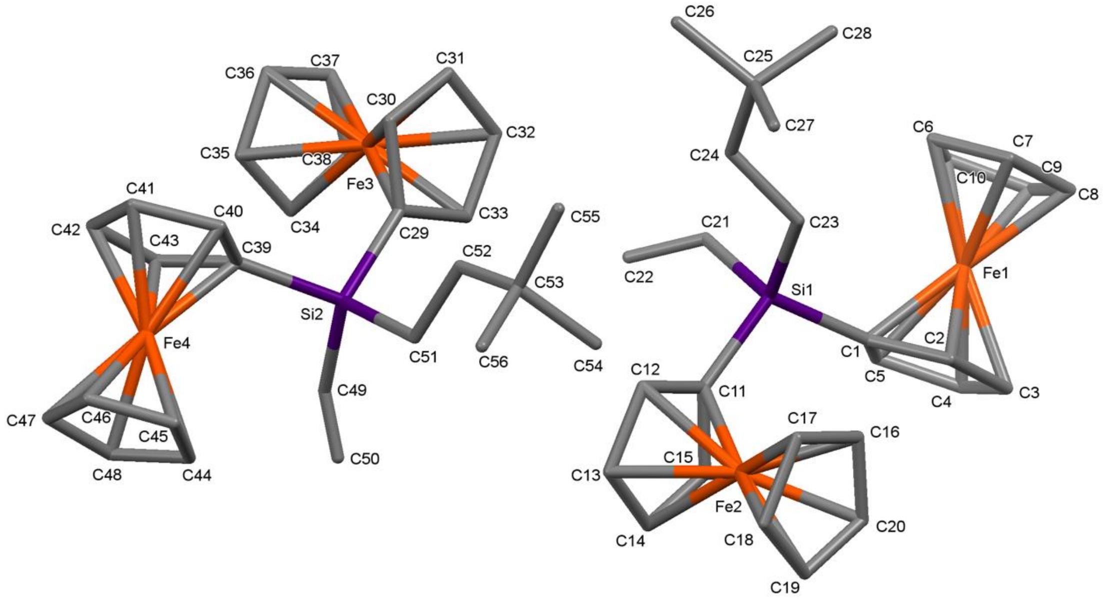

**Figure S26.** Molecular structure of compound **5** with atoms labelled**.** Hydrogen atoms have been removed for clarity.

A total of 3719 frames were collected. The frames were integrated with the Bruker SAINT software package using a narrow-frame algorithm. The integration of the data using a triclinic unit cell yielded a total of 72161 reflections to a maximum θ angle of 25.35° (0.83 Å resolution), of which 9131 were independent (average redundancy 7.903, completeness = 99.1%, $R_{int}$ = 3.66%, $R_{sig}$ = 2.37%) and 7176 (78.59%) were greater than $2\sigma(F^2)$.

*Unit cell*

The final cell constants of *a* = 12.7847(4) Å, *b* = 15.1066(4) Å, *c* = 15.2614(5) Å, α = 96.779(1)°, β = 108.237(2)°, γ = 111.313(1)°, volume = 2516.90(13) $Å^3$, are based upon the refinement of the XYZ-centroids of 150 reflections above 20 σ(I) with 6.510° < 2θ < 52.34°.

*Scaling*

Data were corrected for absorption effects using the multi-scan method (SADABS). The ratio of minimum to maximum apparent transmission was 0.914. The calculated minimum and maximum transmission coefficients (based on crystal size) are 0.7678 and 0.8296.

*Structure solution and refinement*

The structure was solved and refined using the Bruker SHELXTL Software Package, using the space group *P*-1, with Z = 4 for the formula unit, $C_{28}H_{34}Fe_2Si$. The final anisotropic full-matrix least-squares refinement on $F^2$ with 565 variables converged at $R_1$ = 3.90%, for the observed data and $wR_2$ = 14.01% for all data. The goodness-of-fit was 1.000. The largest peak in the final difference electron density synthesis was 0.669 $e^-/Å^3$ and the largest hole was -0.475 $e^-/Å^3$ with an RMS deviation of 0.088 $e^-/Å^3$. On the basis of the final model, the calculated density was 1.347 $g/cm^3$ and F(000), 1072 $e^-$.

**Table S1. Sample and crystal data for 5.**

| | | |
|---|---|---|
| **Chemical formula** | $C_{28}H_{34}Fe_2Si$ | |
| **Formula weight** | 510.34 | |
| **Temperature** | 296(2) K | |
| **Wavelength** | 0.71073 Å | |
| **Crystal size** | 0.16 x 0.18 x 0.23 mm | |
| **Crystal habit** | clear dark orange prismatic | |
| **Crystal system** | triclinic | |
| **Space group** | *P*-1 | |
| **Unit cell dimensions** | *a* = 12.7847(4) Å | α = 96.779(1)° |
| | *b* = 15.1066(4) Å | β = 108.237(2)° |
| | *c* = 15.2614(5) Å | γ = 111.313(1)° |
| **Volume** | 2516.9(1) $Å^3$ | |
| **Z** | 4 | |
| **Density (calculated)** | 1.347 $Mg/cm^3$ | |
| **Absorption coefficient** | 1.213 $mm^{-1}$ | |
| **F(000)** | 1072 | |

**Table S2. Data collection and structure refinement for 5.**

| | |
|---|---|
| **Theta range for data collection** | 1.46 to 25.35° |
| **Index ranges** | -15<=h<=15, -18<=k<=18, -18<=l<=18 |
| **Reflections collected** | 72161 |
| **Independent reflections** | 9131 [R(int) = 0.0366] |
| **Coverage of independent reflections** | 99.1% |
| **Absorption correction** | multi-scan |
| **Max. and min. transmission** | 0.8296 and 0.7678 |
| **Structure solution technique** | direct methods |
| **Structure solution program** | SHELXS-97 (Sheldrick, 2008) |
| **Refinement method** | Full-matrix least-squares on $F^2$ |
| **Refinement program** | SHELXL-97 (Sheldrick, 2008) |
| **Function minimized** | $\Sigma$ w($F_o^2$ - $F_c^2$)$^2$ |
| **Data / restraints / parameters** | 9131 / 0 / 565 |
| **Goodness-of-fit on $F^2$** | 1.000 |
| **Final R indices** | 7176 data; I>2σ(I) $R_1$ = 0.0390, $wR_2$ = 0.1161 |
| | all data $R_1$ = 0.0567, $wR_2$ = 0.1401 |
| **Weighting scheme** | $w$=1/[$\sigma^2(F_o^2)+(0.0908P)^2+1.1624P$]<br>where P=($F_o^2+2F_c^2$)/3 |
| **Largest diff. peak and hole** | 0.669 and -0.475 eÅ$^{-3}$ |
| **R.M.S. deviation from mean** | 0.088 eÅ$^{-3}$ |

### 3.2. Single crystal X-ray diffraction supplementary information for 6

A clear intense orange plate-like specimen of $C_{24}H_{24}Fe_2OSi$, approximate dimensions 0.04 mm x 0.20 mm x 0.24 mm, was used for the X-ray crystallographic analysis. The X-ray intensity data were measured in a Bruker Kappa Apex II diffractometer.

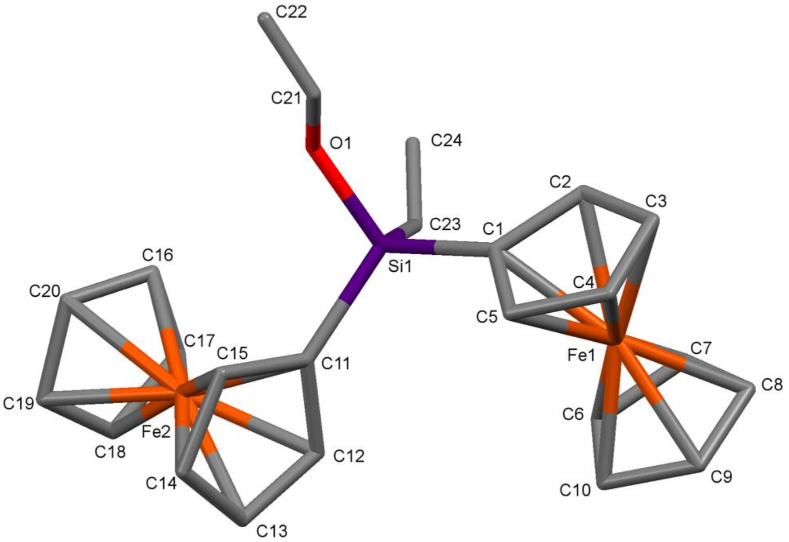

**Figure S27.** Molecular structure of compound **6** with atoms labelled. Hydrogen atoms have been removed for clarity.

A total of 7663 frames were collected. The total exposure time was 63.86 hours. The frames were integrated with the Bruker SAINT software package using a narrow-frame algorithm. The integration of the data using a triclinic unit cell yielded a total of 68641 reflections to a maximum θ angle of 26.41° (0.80 Å resolution), of which 4330 were independent (average redundancy 15.852, completeness = 99.7%, $R_{int}$ = 3.54%, $R_{sig}$ = 1.61%) and 3317 (76.61%) were greater than $2\sigma(F^2)$.

*Unit cell*

The final cell constants of *a* = 7.5488(2) Å, *b* = 11.3227(2) Å, *c* = 12.7162(3) Å, α = 79.503(1)°, β = 84.097(1)°, γ = 82.215(1)°, volume = 1055.44(4) $Å^3$, are based upon the refinement of the XYZ-centroids of 9858 reflections above 20 σ(I) with $4.488° < 2\theta < 46.11°$.

*Scaling*

Data were corrected for absorption effects using the multi-scan method (SADABS). The ratio of minimum to maximum apparent transmission was 0.881. The calculated minimum and maximum transmission coefficients (based on crystal size) are 0.7234 and 0.9445.

*Structure solution and refinement*

The structure was solved and refined using the Bruker SHELXTL Software Package, using the space group *P*-1, with Z = 2 for the formula unit, $C_{24}H_{24}Fe_2OSi$. The final anisotropic full-matrix least-squares refinement on $F^2$ with 253 variables converged at $R_1$ = 3.99%, for the observed data and $wR_2$ = 14.47% for all data. The goodness-of-fit was 1.000. The largest peak in the final difference electron density synthesis was 0.530 $e^-/Å^3$ and the largest hole was -0.421 $e^-/Å^3$ with an RMS deviation of 0.073 $e^-/Å^3$. On the basis of the final model, the calculated density was 1.473 $g/cm^3$ and F(000), 484 $e^-$.

**Table S3. Sample and crystal data for 6.**

| | | |
|---|---|---|
| **Chemical formula** | $C_{24}H_{24}Fe_2OSi$ | |
| **Formula weight** | 468.22 | |
| **Temperature** | 296(2) K | |
| **Wavelength** | 0.71073 Å | |
| **Crystal size** | 0.04 x 0.20 x 0.24 mm | |
| **Crystal habit** | clear intense orange plate | |
| **Crystal system** | triclinic | |
| **Space group** | *P*-1 | |
| **Unit cell dimensions** | *a* = 7.5488(2) Å | α = 79.503(1)° |
| | *b* = 11.3227(2) Å | β = 84.097(1)° |
| | *c* = 12.7162(3) Å | γ = 82.215(1)° |
| **Volume** | 1055.44(4) $Å^3$ | |
| **Z** | 2 | |
| **Density (calculated)** | 1.473 $Mg/cm^3$ | |
| **Absorption coefficient** | 1.443 $mm^{-1}$ | |
| **F(000)** | 484 | |

**Table S4. Data collection and structure refinement for 6.**

| | |
|---|---|
| **Theta range for data collection** | 1.63 to 26.41° |
| **Index ranges** | -9<=h<=9, -14<=k<=13, -15<=l<=15 |
| **Reflections collected** | 68641 |
| **Independent reflections** | 4330 [R(int) = 0.0354] |
| **Coverage of independent reflections** | 99.7% |
| **Absorption correction** | multi-scan |
| **Max. and min. transmission** | 0.9445 and 0.7234 |
| **Structure solution technique** | direct methods |
| **Structure solution program** | SHELXS-97 (Sheldrick, 2008) |
| **Refinement method** | Full-matrix least-squares on $F^2$ |
| **Refinement program** | SHELXL-97 (Sheldrick, 2008) |
| **Function minimized** | $\Sigma$ w($F_o^2$ - $F_c^2$)$^2$ |
| **Data / restraints / parameters** | 4330 / 0 / 253 |
| **Goodness-of-fit on $F^2$** | 1.000 |
| **Final R indices** | 3317 data; I>2σ(I) $R_1$ = 0.0399, $wR_2$ = 0.1199 |
| | all data $R_1$ = 0.0584, $wR_2$ = 0.1447 |
| **Weighting scheme** | $w=1/[\sigma^2(F_o^2)+(0.0869P)^2+0.7263P]$<br>where $P=(F_o^2+2F_c^2)/3$ |
| **Largest diff. peak and hole** | 0.530 and -0.421 eÅ$^{-3}$ |
| **R.M.S. deviation from mean** | 0.073 eÅ$^{-3}$ |

### 3.3. Single crystal X-ray diffraction supplementary information for 7

A clear intense orange plate-like specimen of $C_{22}H_{22}Fe_2OSi$, approximate dimensions 0.02 mm x 0.19 mm x 0.38 mm, was used for the X-ray crystallographic analysis. The X-ray intensity data were measured in a Bruker Kappa Apex II diffractometer.

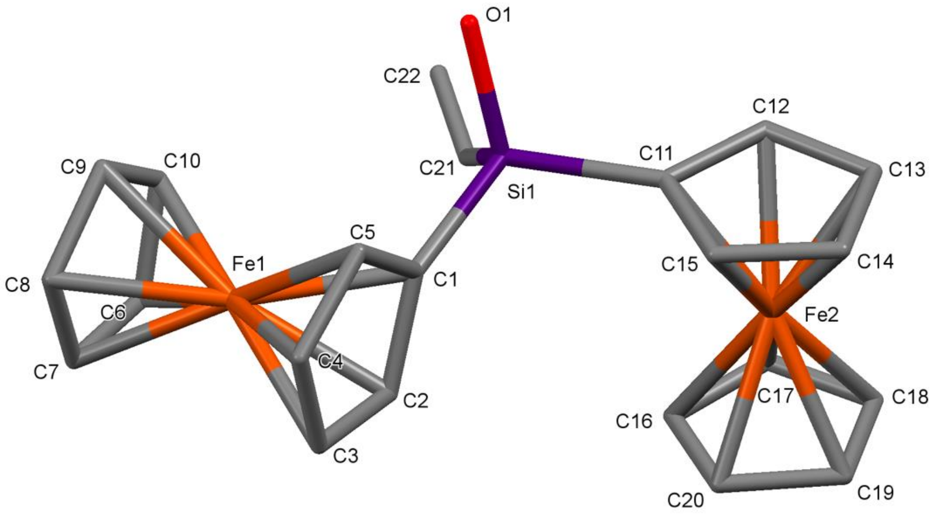

**Figure S28.** Molecular structure of compound **7** with atoms labelled**.** Hydrogen atoms have been removed for clarity.

A total of 3884 frames were collected. The total exposure time was 16.18 hours. The frames were integrated with the Bruker SAINT software package using a narrow-frame algorithm. The integration of the data using a triclinic unit cell yielded a total of 23251 reflections to a maximum θ angle of 25.35° (0.83 Å resolution), of which 3514 were independent (average redundancy 6.617, completeness = 99.9%, $R_{int}$ = 2.89%, $R_{sig}$ = 1.90%) and 2945 (83.81%) were greater than $2\sigma(F^2)$.

*Unit cell*

The final cell constants of *a* = 7.54800(10) Å, *b* = 10.8128(2) Å, *c* = 12.8883(2) Å, α = 71.763(1)°, β = 74.408(1)°, γ = 86.198(1)°, volume = 962.10(3) Å$^3$, are based upon the refinement of the XYZ-centroids of 9576 reflections above 20 σ(I) with 4.384° < 2θ < 52.74°.

*Scaling*

Data were corrected for absorption effects using the multi-scan method (SADABS). The ratio of minimum to maximum apparent transmission was 0.855. The calculated minimum and maximum transmission coefficients (based on crystal size) are 0.5855 and 0.9691.

*Structure solution and refinement*

The structure was solved and refined using the Bruker SHELXTL Software Package, using the space group *P*-1, with Z = 2 for the formula unit, $C_{22}H_{22}Fe_2OSi$. The final anisotropic full-matrix least-squares refinement on $F^2$ with 236 variables converged at $R_1$ = 3.13%, for the observed data and $wR_2$ = 12.21% for all data. The goodness-of-fit was 1.000. The largest peak in the final difference electron density synthesis was 0.559 e$^-$/Å$^3$ and the largest hole was -0.570 e$^-$/Å$^3$ with an RMS deviation of 0.090 e$^-$/Å$^3$. On the basis of the final model, the calculated density was 1.526 g/cm$^3$ and F(000), 456 e$^-$.

**Table S5. Sample and crystal data for 7.**

| | | |
|---|---|---|
| **Chemical formula** | $C_{22}H_{22}Fe_2OSi$ | |
| **Formula weight** | 442.19 | |
| **Temperature** | 296(2) K | |
| **Wavelength** | 0.71073 Å | |
| **Crystal size** | 0.02 x 0.19 x 0.38 mm | |
| **Crystal habit** | clear intense orange plate | |
| **Crystal system** | triclinic | |
| **Space group** | *P*-1 | |
| **Unit cell dimensions** | *a* = 7.54800(10) Å | α = 71.763(1)° |
| | *b* = 10.8128(2) Å | β = 74.408(1)° |
| | *c* = 12.8883(2) Å | γ = 86.198(1)° |
| **Volume** | 962.10(3) Å$^3$ | |
| **Z** | 2 | |
| **Density (calculated)** | 1.526 Mg/cm$^3$ | |
| **Absorption coefficient** | 1.578 mm$^{-1}$ | |
| **F(000)** | 456 | |

**Table S6. Data collection and structure refinement for 8.**

| | |
|---|---|
| **Theta range for data collection** | 1.72 to 25.35° |
| **Index ranges** | -9<=h<=9, -12<=k<=13, -15<=l<=15 |
| **Reflections collected** | 23251 |
| **Independent reflections** | 3514 [R(int) = 0.0289] |
| **Coverage of independent reflections** | 99.9% |
| **Absorption correction** | multi-scan |
| **Max. and min. transmission** | 0.9691 and 0.5855 |
| **Structure solution technique** | direct methods |
| **Structure solution program** | SHELXS-97 (Sheldrick, 2008) |
| **Refinement method** | Full-matrix least-squares on $F^2$ |
| **Refinement program** | SHELXL-97 (Sheldrick, 2008) |
| **Function minimized** | $\Sigma\ w(F_o^2 - F_c^2)^2$ |
| **Data / restraints / parameters** | 3514 / 0 / 236 |
| **Goodness-of-fit on $F^2$** | 1.000 |
| **Final R indices** | 2945 data; I>2σ(I) $R_1 = 0.0313$, $wR_2 = 0.0956$ |
| | all data $R_1 = 0.0422$, $wR_2 = 0.1221$ |
| **Weighting scheme** | $w=1/[\sigma^2(F_o^2)+(0.0877P)^2+0.4271P]$<br>where $P=(F_o^2+2F_c^2)/3$ |
| **Largest diff. peak and hole** | 0.559 and -0.570 eÅ$^{-3}$ |
| **R.M.S. deviation from mean** | 0.090 eÅ$^{-3}$ |

## 3.4. Single crystal X-ray diffraction supplementary information for 8

A clear orange prismatic-like specimen of $C_{44}H_{42}Fe_4O_3Si_2$, approximate dimensions 0.21 mm x 0.35 mm x 0.40 mm, was used for the X-ray crystallographic analysis. The X-ray intensity data were measured in a Bruker Kappa Apex II diffractometer.

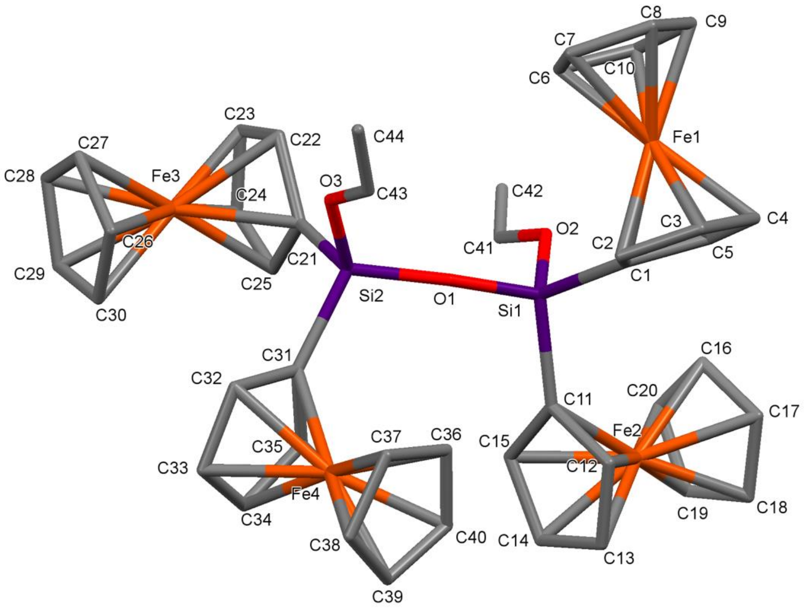

**Figure S29.** Molecular structure of compound **8** with atoms labelled**.** Hydrogen atoms have been removed for clarity.

A total of 3081 frames were collected. The total exposure time was 17.12 hours. The frames were integrated with the Bruker SAINT software package using a narrow-frame algorithm. The integration of the data using a monoclinic unit cell yielded a total of 110301 reflections to a maximum θ angle of 25.35° (0.83 Å resolution), of which 7005 were independent (average redundancy 15.746, completeness = 100.0%, $R_{int}$ = 4.11%, $R_{sig}$ = 1.60%) and 6110(87.22%) were greater than $2\sigma(F^2)$.

*Unit cell*

The final cell constants of *a* = 12.9028(4) Å, *b* = 21.3942(6) Å, *c* = 14.7802(4) Å, β = 110.413(1)°, volume = 3823.79(19) $Å^3$, are based upon the refinement of the XYZ-centroids of 9861 reflections above 20 σ(I) with 4.811° < 2θ < 52.72°.

*Scaling*

Data were corrected for absorption effects using the multi-scan method (SADABS). The ratio of minimum to maximum apparent transmission was 0.811. The calculated minimum and maximum transmission coefficients (based on crystal size) are 0.5900 and 0.7300.

*Structure solution and refinement*

The structure was solved and refined using the Bruker SHELXTL Software Package, using the space group $P2_1/n$, with Z = 4 for the formula unit, $C_{44}H_{42}Fe_4O_3Si_2$. The final anisotropic full-matrix least-squares refinement on $F^2$ with 478 variables converged at $R_1$ = 2.68%, for the observed data and $wR_2$ = 10.83% for all data. The goodness-of-fit was 1.004. The largest peak in the final difference electron density synthesis was 0.392 $e^-/Å^3$ and the largest hole was -0.311 $e^-/Å^3$ with an RMS deviation of 0.092 $e^-/Å^3$. On the basis of the final model, the calculated density was 1.561 $g/cm^3$ and F(000), 1848 $e^-$.

**Table S7. Sample and crystal data for 8.**

| | | |
|---|---|---|
| **Chemical formula** | $C_{44}H_{42}Fe_4O_3Si_2$ | |
| **Formula weight** | 898.36 | |
| **Temperature** | 296(2) K | |
| **Wavelength** | 0.71073 Å | |
| **Crystal size** | 0.21 x 0.35 x 0.40 mm | |
| **Crystal habit** | clear orange prismatic | |
| **Crystal system** | monoclinic | |
| **Space group** | $P2_1/n$ | |
| **Unit cell dimensions** | *a* = 12.9028(4) Å | α = 90° |
| | *b* = 21.3942(6) Å | β = 110.413(1)° |
| | *c* = 14.7802(4) Å | γ = 90° |
| **Volume** | 3823.79(19) $Å^3$ | |
| **Z** | 4 | |
| **Density (calculated)** | 1.561 $Mg/cm^3$ | |
| **Absorption coefficient** | 1.591 $mm^{-1}$ | |
| **F(000)** | 1848 | |

**Table S8. Data collection and structure refinement for SoniaBrunna00678c.**

| | | |
|---|---|---|
| **Theta range for data collection** | 1.75 to 25.35° | |
| **Index ranges** | -15<=h<=15, -25<=k<=25, -17<=l<=17 | |
| **Reflections collected** | 110301 | |
| **Independent reflections** | 7005 [R(int) = 0.0411] | |
| **Coverage of independent reflections** | 100.0% | |
| **Absorption correction** | multi-scan | |
| **Max. and min. transmission** | 0.7300 and 0.5900 | |
| **Structure solution technique** | direct methods | |
| **Structure solution program** | SHELXS-97 (Sheldrick, 2008) | |
| **Refinement method** | Full-matrix least-squares on $F^2$ | |
| **Refinement program** | SHELXL-97 (Sheldrick, 2008) | |
| **Function minimized** | $\Sigma$ w($F_o^2$ - $F_c^2$)$^2$ | |
| **Data / restraints / parameters** | 7005 / 0 / 478 | |
| **Goodness-of-fit on $F^2$** | 1.004 | |
| **Final R indices** | 6110 data; I>2σ(I) | $R_1$ = 0.0268, $wR_2$ = 0.0852 |
| | all data | $R_1$ = 0.0351, $wR_2$ = 0.1083 |
| **Weighting scheme** | $w=1/[\sigma^2(F_o^2)+(0.0793P)^2+1.4351P]$<br>where $P=(F_o^2+2F_c^2)/3$ | |
| **Largest diff. peak and hole** | 0.392 and -0.311 eÅ$^{-3}$ | |
| **R.M.S. deviation from mean** | 0.092 eÅ$^{-3}$ | |

### 3.5. Single crystal X-ray diffraction supplementary information for 9

A clear orange prismatic-like specimen of $C_{52}H_{48}Fe_5O_2Si_2$, approximate dimensions 0.14 mm x 0.20 mm x 0.21 mm, was used for the X-ray crystallographic analysis. The X-ray intensity data were measured in a Bruker Kappa Apex II diffractometer.

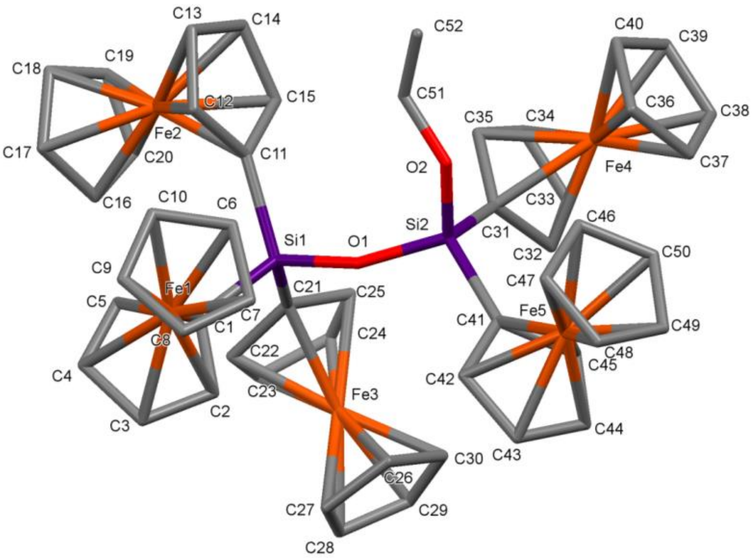

**Figure S30.** Molecular structure of compound **9** with atoms labelled**.** Hydrogen atoms have been removed for clarity.

A total of 1557 frames were collected. The total exposure time was 25.95 hours. The frames were integrated with the Bruker SAINT software package using a narrow-frame algorithm. The integration of the data using a triclinic unit cell yielded a total of 25839 reflections to a maximum θ angle of 25.35° (0.83 Å resolution), of which 7946 were independent (average redundancy 3.252, completeness = 98.1%, $R_{int}$ = 6.22%, $R_{sig}$ = 6.92%) and 5464 (68.76%) were greater than 2σ($F^2$).

*Unit cell*

The final cell constants of *a* = 11.039(2) Å, *b* = 11.451(1) Å, *c* = 17.549(2) Å, α = 92.680(5)°, β = 90.194(5)°, γ = 90.255(5)°, volume = 2215.8(5) $Å^3$, are based upon the refinement of the XYZ-centroids of 5648 reflections above 20 σ(I) with 5.140° < 2θ < 47.34°.

*Scaling*

Data were corrected for absorption effects using the multi-scan method (SADABS). The ratio of minimum to maximum apparent transmission was 0.750. The calculated minimum and maximum transmission coefficients (based on crystal size) are 0.7175 and 0.7974.

*Structure solution and refinement*

The structure was solved and refined using the Bruker SHELXTL Software Package, using the space group *P*-1, with Z = 2 for the formula unit, $C_{52}H_{48}Fe_5O_2Si_2$. The final anisotropic full-matrix least-squares refinement on $F^2$ with 550 variables converged at $R_1$ = 5.36%, for the observed data and $wR_2$ = 17.14% for all data. The goodness-of-fit was 1.080. The largest peak in the final difference electron density synthesis was 0.864 $e^-/Å^3$ and the largest hole was -1.102 $e^-/Å^3$ with an RMS deviation of 0.214 $e^-/Å^3$. On the basis of the final model, the calculated density was 1.559 g/$cm^3$ and F(000), 1068 $e^-$.

**Table S9. Sample and crystal data for 9.**

| | | |
|---|---|---|
| **Chemical formula** | $C_{52}H_{48}Fe_5O_2Si_2$ | |
| **Formula weight** | 1040.33 | |
| **Temperature** | 296(2) K | |
| **Wavelength** | 0.71073 Å | |
| **Crystal size** | 0.14 x 0.20 x 0.21 mm | |
| **Crystal habit** | clear orange prismatic | |
| **Crystal system** | triclinic | |
| **Space group** | *P*-1 | |
| **Unit cell dimensions** | *a* = 11.039(2) Å | α = 92.680(5)° |
| | *b* = 11.451(1) Å | β = 90.194(5)° |
| | *c* = 17.549(2) Å | γ = 90.255(5)° |
| **Volume** | 2215.8(5) $Å^3$ | |
| **Z** | 2 | |
| **Density (calculated)** | 1.559 Mg/$cm^3$ | |
| **Absorption coefficient** | 1.694 $mm^{-1}$ | |
| **F(000)** | 1068 | |

**Table S10. Data collection and structure refinement for 9.**

| | |
|---|---|
| **Theta range for data collection** | 1.78 to 25.35° |
| **Index ranges** | -13<=h<=13, -13<=k<=11, -21<=l<=21 |
| **Reflections collected** | 25839 |
| **Independent reflections** | 7946 [R(int) = 0.0622] |
| **Coverage of independent reflections** | 98.1% |
| **Absorption correction** | multi-scan |
| **Max. and min. transmission** | 0.7974 and 0.7175 |
| **Structure solution technique** | direct methods |
| **Structure solution program** | SHELXS-97 (Sheldrick, 2008) |
| **Refinement method** | Full-matrix least-squares on $F^2$ |
| **Refinement program** | SHELXL-97 (Sheldrick, 2008) |
| **Function minimized** | $\Sigma\ w(F_o^2 - F_c^2)^2$ |
| **Data / restraints / parameters** | 7946 / 0 / 550 |
| **Goodness-of-fit on $F^2$** | 1.080 |
| **Final R indices** | 5464 data; $I>2\sigma(I)$ $R_1 = 0.0536$, $wR_2 = 0.1288$ |
| | all data $R_1 = 0.0914$, $wR_2 = 0.1714$ |
| **Weighting scheme** | $w=1/[\sigma^2(F_o^2)+(0.0985P)^2+0.0000P]$<br>where $P=(F_o^2+2F_c^2)/3$ |
| **Largest diff. peak and hole** | 0.864 and -1.102 eÅ$^{-3}$ |
| **R.M.S. deviation from mean** | 0.214 eÅ$^{-3}$ |

**Table S11. Intramolecular Fe-Fe distances in compounds 5-9.**

| | | Distances (Å) | | | |
|---|---|---|---|---|
| **5** | Fe1-Fe2 | 6.0556(8) | Fe3-Fe4 | 6.1853(8) |
| **6** | Fe1-Fe2 | 6.085(6) | | |
| **7** | Fe1-Fe2 | 6.1174(6) | | |
| **8** | Fe1-Fe2 | 6.1052(5) | Fe2-Fe3 | 8.4029(6) |
| | Fe1-Fe3 | 8.1369(6) | Fe2-Fe4 | 6.3853(7) |
| | Fe1-Fe4 | 7.3512(7) | Fe3-Fe4 | 5.9037(5) |
| | Fe1-Fe2 | 5.480(1) | Fe2-Fe4 | 7.465(1) |
| | Fe1-Fe3 | 6.077(1) | Fe2-Fe5 | 9.327(1) |

|  |  |  |  |  |
|---|---|---|---|---|
| **9** | Fe1-Fe4 | 8.567(1) | Fe3-Fe4 | 6.501(1) |
|  | Fe1-Fe5 | 6.751(1) | Fe3-Fe5 | 7.114(1) |
|  | Fe2-Fe3 | 6.056(1) | Fe4-Fe5 | 5.444(1) |

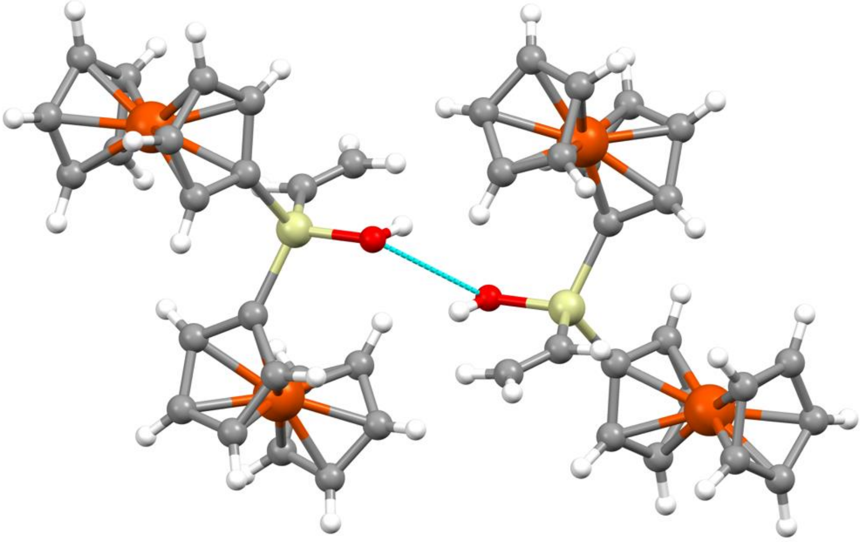

**Figure S31.** Hydrogen bond (in cyan) between hydroxyl groups in compound **7**.

## Table S12. Hydrogen bond parameters in compound 7.

|  | **Donor-H (Å)** | **Acceptor-H(Å)** | **Donor-Acceptor(Å)** | **Angle (°)** |
|---|---|---|---|---|
| **O1-H···O1(-x+1, -y+1, -z)** | 0.82 | 2.29 | 2.811(5) | 121.7 |

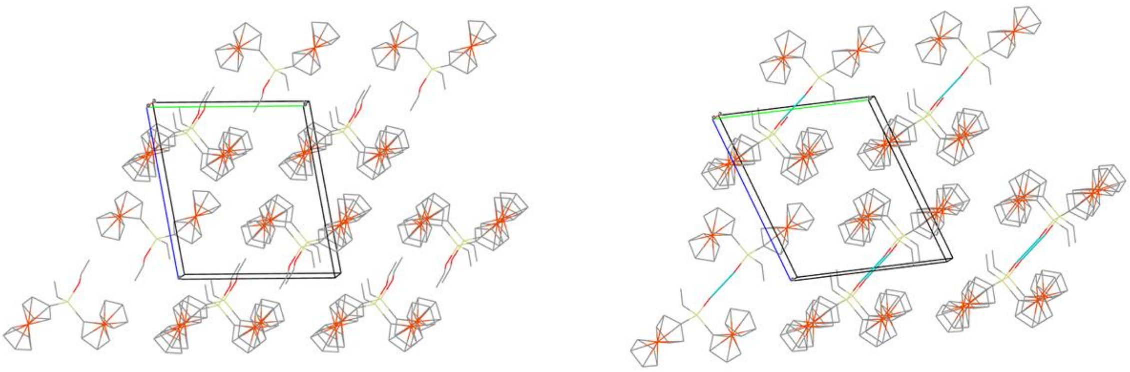

**Figure S32.** View along the a axis of the packing of compounds **6** and **7**; hydrogen bonds in **7** are depicted in cyan.

## Table S13. Relevant bond distances and angles in compounds 5-9.

**Bond distances (Å)**

| | | | | |
|---|---|---|---|---|
| **5** | Si1-C1 | 1.872(3) | Si2-C29 | 1.868(3) |
| | Si1-C11 | 1.859(3) | Si2-C39 | 1.859(4) |
| | Si1-C21 | 1.868(3) | Si2-C49 | 1.853(5) |
| | Si1-C23 | 1.877(3) | Si2-C51 | 1.881(4) |
| **6** | Si1-C1 | 1.855(4) | Si1-C23 | 1.794(7) |
| | Si1-C11 | 1.848(4) | Si1-O1 | 1.654(4) |
| **7** | Si1-C1 | 1.841(3) | Si1-C21 | 1.856(5) |
| | Si1-C11 | 1.856(3) | Si1-O1 | 1.650(3) |
| **8** | Si1-C1 | 1.840(2) | Si2-C21 | 1.839(2) |
| | Si1-C11 | 1.840(3) | Si2-C31 | 1.840(3) |
| | Si1-O1 | 1.620(2) | Si2-O1 | 1.620(2) |
| | Si1-O2 | 1.642(2) | Si2-O2 | 1.637(2) |
| **9** | Si1-C1 | 1.851(5) | Si2-C31 | 1.842(5) |
| | Si1-C11 | 1.860(3) | Si2-C41 | 1.830(5) |
| | Si1-C21 | 1.851(5) | Si2-O1 | 1.616(3) |
| | Si1-O1 | 1.638(3) | Si2-O2 | 1.652(4) |

**Bond angles (°)**

| | | | | |
|---|---|---|---|---|
| **5** | C1-Si1-C11 | 109.2(1) | C29-Si2-C39 | 109.6(2) |
| | C1-Si1-C21 | 107.2(2) | C29-Si2-C49 | 108.9(2) |
| | C1-Si1-C23 | 111.2(1) | C29-Si2-C51 | 106.9(2) |
| | C11-Si1-C21 | 108.0(2) | C39-Si2-C49 | 109.4(2) |
| | C11-Si1-C23 | 110.7(2) | C39-Si2-C51 | 111.3(2) |
| | C21-Si1-C23 | 110.4(2) | C49-Si2-C51 | 109.8(2) |
| **6** | C1-Si1-C11 | 110.3(2) | C11-Si1-C23 | 111.7(2) |
| | C1-Si1-C23 | 111.2(2) | C11-Si1-O1 | 109.1(2) |
| | C1-Si1-O1 | 110.1(2) | C23-Si1-O1 | 104.4(3) |
| **7** | C1-Si1-C11 | 108.9(2) | C11-Si1-C21 | 111.9(2) |
| | C1-Si1-C21 | 112.1(2) | C11-Si1-O1 | 105.7(2) |
| | C1-Si1-O1 | 107.9(2) | C21-Si1-O1 | 110.1(2) |
| **8** | C1-Si1-C11 | 109.5(1) | C21-Si2-C31 | 109.1(1) |
| | C1-Si1-O1 | 110.3(1) | C21-Si2-O1 | 111.5(1) |
| | C1-Si1-O2 | 106.7(1) | C21-Si2-O3 | 105.1(1) |
| | C11-Si1-O1 | 109.3(1) | C31-Si2-O1 | 111.2(1) |
| | C11-Si1-O2 | 112.3(1) | C31-Si2-O3 | 111.2(1) |
| | O1-Si1-O2 | 108.8(1) | O1-Si2-O3 | 108.6(1) |
| **9** | C1-Si1-C11 | 111.4(2) | C31-Si2-C41 | 113.3(2) |
| | C1-Si1-C21 | 111.0(2) | C31-Si2-O1 | 109.4(2) |
| | C1-Si1-O1 | 108.8(2) | C31-Si2-O2 | 110.0(2) |
| | C11-Si1-C21 | 109.7(2) | C41-Si2-O1 | 107.6(2) |
| | C11-Si1-O1 | 108.2(2) | C41-Si2-O2 | 109.0(2) |
| | C21-Si1-O1 | 111.0(2) | O1-Si2-O2 | 107.4(2) |

## 4. Theoretical studies of Compounds 5-7

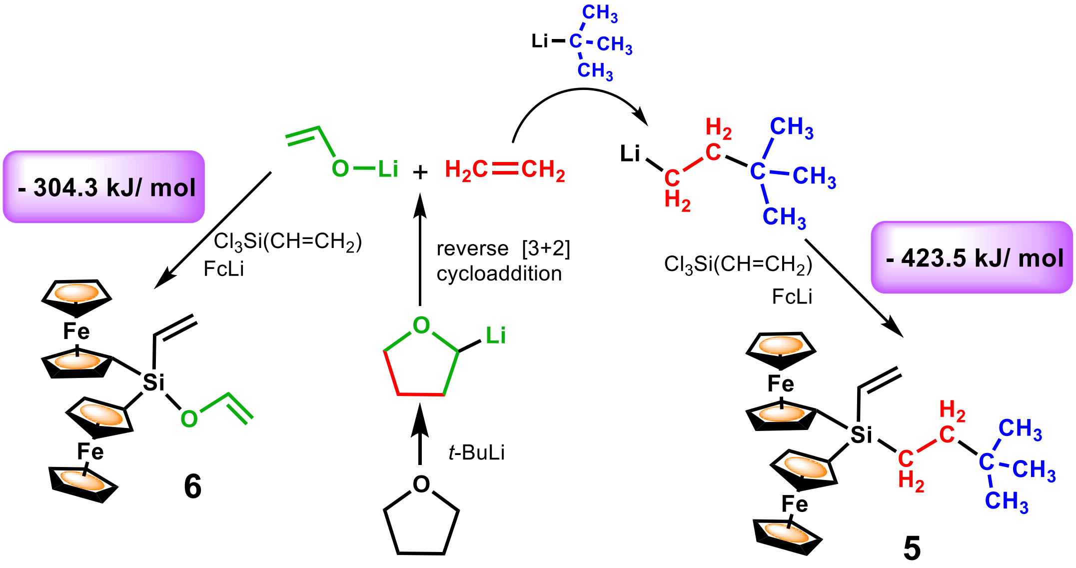

**Figure S33**. Free energy values (kJ/mol) for the stecheometric reactions giving place to compounds **5** and **6**. Both reactions in vacuum are thermodynamically favored from the fragments resulting from the THF cleavage.

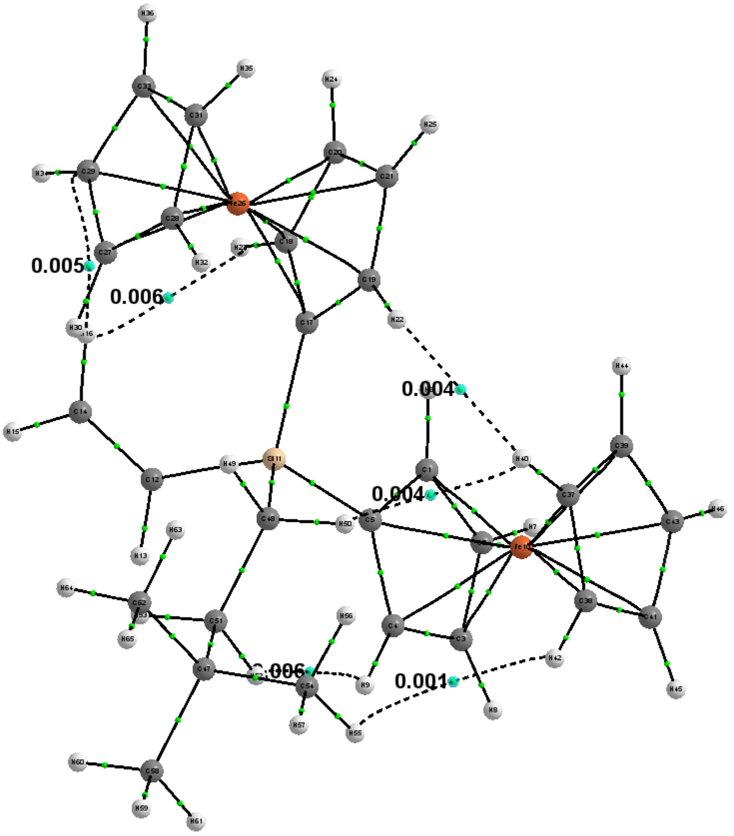

**Figure S34.** Molecular graph for Compound **5** obtained with Quantum Theory of Atoms in Molecules (QTAIM) showing only weak non-covalent interactions between ferrocenyl units and substituents.

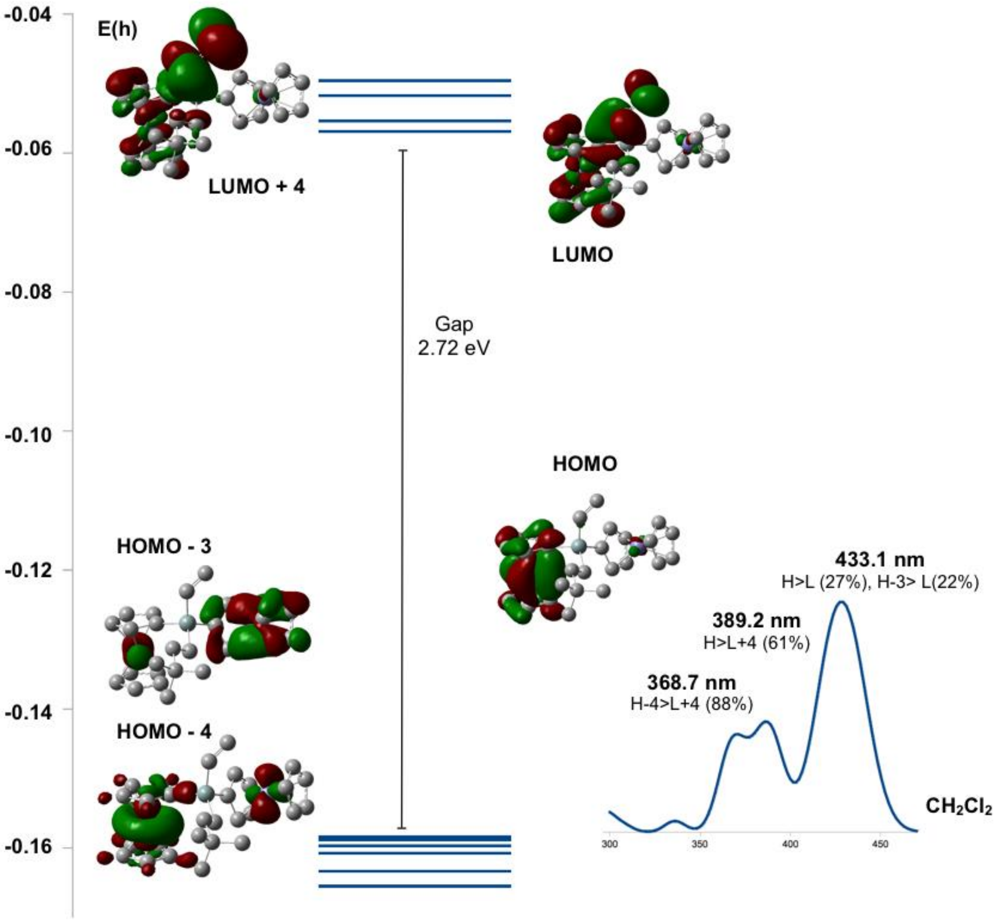

**Figure S35.** Compound **5:** orbital energies (hartrees), HOMO-LUMO gap (eV) and UV-Vis spectrum at the BPW91/6-31+G(d) level of theory obtained by TD-DFT+PCM ($CH_2Cl_2$) calculations (see also Table **S14**).

**Table S14.** List of peaks from the theoretical UV-Vis spectrum of neutral Compound **5** (only oscillator strengths f > 0.0010 are shown) along with their corresponding orbital contributions. Orbital contributions below 10% are omitted for the sake of clarity. Main peaks are in bold characters and illustrated in Figure **S35**. Calculations were carried out with TD-DFT+PCM ($CH_2Cl_2$) at the BPW91/6-31+G(d) level of theory.

| | |
|---|---|
| 439.8 nm, 2.82 eV, f = 0.0018 | H-1->L+1 (+71%) H-1->L (+16%) |
| 434.7 nm, 2.85 eV, f = 0.0019 | H ->L (+33%) H-1->L (30%) |
| **433.1 nm, 2.86 eV, f = 0.0034** | **H ->L (+27%) H-3->L (22%), H-1->L (+17%)** |
| 426.2 nm, 2.91 eV, f = 0.0014 | H ->L+2(+69%) H-2->L+1(11%) |
| 424.9 nm, 2.92 eV, f = 0.0017 | H-3->L+1(+43%) H-2->L+2(+22%) |
| 423.4 nm, 2.93 eV, f = 0.0016 | H-1->L+2(+30%) H-4->L (22%)<br>H-2->L+2(+15%) H-3->L+1(+11%) |
| 419.8 nm, 2.95 eV, f = 0.0013 | H-4->L+1(+71%) H-3->L+2(13%) |
| 417.3 nm, 2.97 eV, f = 0.0017 | H-5->L (+82%) |
| **389.2 nm, 3.19 eV, f = 0.0047** | **H -> L+4 (+61%) H-1 -> L+3(19%)** |
| 379.8 nm, 3.26 eV, f = 0.0010 | H-2->L+4(+97%) |
| **368.7 nm, 3.36 eV, f = 0.0037** | **H-4->L+4 (+88%)** |
| 362.5 nm, 3.42 eV, f = 0.0012 | H-5->L+4(+96%) |

A peak around 450 nm is characteristic from ferrocenyl compounds. For compound **5**, a main peak at 433.1 nm is found, involving three different orbital transitions. Note that the HOMO and HOMO-n (n = 1, 2, 3) orbitals are very close in energy. Interestingly, unoccupied orbitals LUMO and LUMO+4 (see Figure **S35**), which are involved in the most relevant transitions of the spectrum, present a remarkable contribution of the vinyl substituent.